# Supplementary Information

## Characterization procedures

*Phase measurement* was carried out on an X-ray diffractometer **(**Rigaku D/MAX 2200PC) using Ni-filtered Cu Kα radiation at 40 kV and 30 mA. *UV-Vis DRS* was recorded at the wavelength range of 200-900 nm on a Shimazu UV-2700i spectrophotometer using solid $BaSO_4$ powder for background correction. *Textural parameter* measurements were carried out on a surface analyzer **(**JW-BK132F) using $N_2$ physicoadsorption. A sample of 200 mg was degassed at 250 °C for 4 h before measurement. The specific surface area was obtained using the Brunauer-Emmett-Teller (BET) model. Pore volume and pore distribution were obtained using the Barrett-Joyner-Halenda (BJH) model. *Micro morphology* was observed on a FESEM (ZEISS Gemini 300 microscope) at 30 kV and a TEM (FEI Talos F200X) at 200 kV. *XPS* was performed on a Thermo Scientific K-Alpha spectrometer using an Al Kα X-ray radiation source. The base pressure of the chamber was less than $5\times10^{-8}$ Pa. The binding energy (B.E.) was calibrated to adventitious carbon using the C1s peak at 284.8 eV. *$NH_3$-TPD* was performed on a TP-5080 adsorption instrument. A sample of 50 mg was pretreated in a He flow (30 mL·min$^{-1}$) at 550 °C for 1 h and then cooled down to ambient temperature. Then $NH_3$ was adsorbed at 100 °C for 30 min followed by purge in the He flow for 0.5 h. The desorption of $NH_3$ was recorded using TCD as the temperature was raised at 10 °C·min$^{-1}$ from ambient temperature to 600 °C. *$CO_2$/$C_3H_8$-TPD* was carried out on a chemisorption instrument (Micromeritics AutoChem II 2920). A sample of 50 mg was placed into a U-shaped quartz tube and pretreated at 350 °C for 1 h in a He flow (30 mL·min$^{-1}$). Then the sample was cooled down to 50 °C and adsorbed $CO_2$/$C_3H_8$ (30 mL·min$^{-1}$) for 30 min. Next, the sample was purged by the He flow for 1 h. Subsequently, as the temperature rose to 800 °C at a rate of 10 °C·min$^{-1}$, the desorption amount of $CO_2$/$C_3H_8$ was recorded using TCD. For *$H_2$-TPR*, a sample of 50 mg was loaded into, followed by pretreatment at 300 °C for 1 h, and cooled down to ambient temperature in the He flow. Then, as the sample was heated at 10 °C·min$^{-1}$ to 800 °C in a 10% $H_2$/Ar flow (30 mL·min$^{-1}$), the $H_2$ consumed was recorded. *TG analysis* of the used catalyst samples was carried out on a thermogravimetric analyzer (NETZSCH STA 449). A sample of 20 mg was heated at 20 °C·min$^{-1}$ from ambient temperature to 800 °C in an air flow (30 mL·min$^{-1}$), and the weight was synchronously recorded. *Raman spectra* were recorded on a HORIBA Scientific LabRAM HR Evolution spectrophotometer equipped with a solid state laser (532 nm wave-length, 17 mW capacity) as the

excitation source and a 5x objective lens, at ambient temperature in the wavenumber range of 100−2000 $cm^{-1}$. *In-situ DRIFTS analysis* was carried out on a Bruker Tensor II spectrometer equipped with a diffuse reflectance cell. The catalyst sample was pretreated at 300 °C in an Ar flow (20 $mL \cdot min^{-1}$) for 2 h, and cooled down to 30 °C. The background was recorded. Then $C_3H_8$-$CO_2$ (1/1, 20 $mL \cdot min^{-1}$) was switched into. As the cell was heated at 10 $°C \cdot min^{-1}$, the spectra at the set temperature interval were collected.

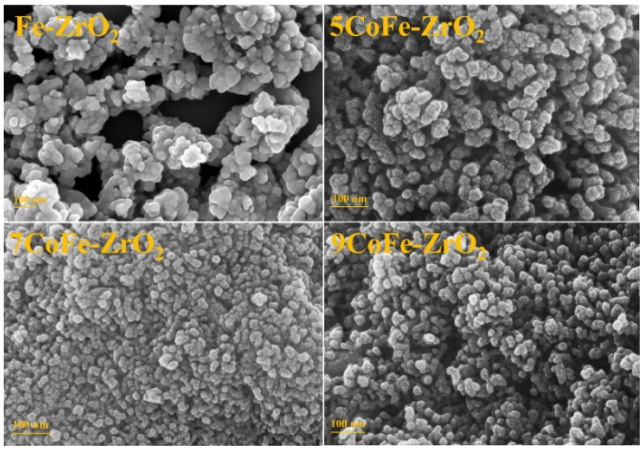


**Fig. S1** SEM images of fresh catalysts.

**Table S1** Textural parameters of fresh catalysts

| Catalysts | $A_{BET}$ ($m^2 \cdot g^{-1}$) | Cumulative pore volume($cm^3 \cdot g^{-1}$) | Average pore diameter(nm) |
|---|---|---|---|
| Fe-$ZrO_2$ | 63.9 | 0.30 | 10.9 |
| 3CoFe-$ZrO_2$ | 87.6 | 0.26 | 8.3 |
| 5CoFe-$ZrO_2$ | 87.9 | 0.25 | 9.4 |
| 7CoFe-$ZrO_2$ | 88.3 | 0.25 | 8.7 |
| 9CoFe-$ZrO_2$ | 89.6 | 0.24 | 8.4 |

**Table S2** Initial catalytic activity of nCoFe-$ZrO_2$ for propane and $CO_2$ reaction

| Catalysts | Conv. (%) | | Hydrocarbon sel. (%) | | | | Yield (%) | | | Carbon balance (%) |
|---|---|---|---|---|---|---|---|---|---|---|
| | $C_3H_8$ | $CO_2$ | $C_3H_6$ | $CH_4$ | $C_2H_4$ | $C_2H_6$ | $C_3H_6$ | CO | $H_2$ | |
| Co-$ZrO_2$ | 77.1 | 57.8 | 0 | 100 | 0 | 0 | 0 | 54.5 | 41.8 | 65.0 |
| 9CoFe-$ZrO_2$ | 48.1 | 38.2 | 75.6 | 18.7 | 1.34 | 0.64 | 36.4 | 31.7 | 6.87 | 95.7 |
| 7CoFe-$ZrO_2$ | 47.6 | 37.4 | 80.1 | 15.2 | 1.82 | 0.59 | 38.1 | 29.5 | 6.94 | 97.1 |
| 5CoFe-$ZrO_2$ | 45.8 | 36.6 | 81.2 | 12.1 | 2.34 | 0.56 | 37.2 | 26.1 | 6.45 | 95.8 |
| 3CoFe-$ZrO_2$ | 45.1 | 35.9 | 82.7 | 10.8 | 2.11 | 0.51 | 37.3 | 25.6 | 5.85 | 94.4 |
| Fe-$ZrO_2$ | 39.9 | 28.2 | 83.7 | 7.55 | 1.61 | 0.42 | 33.1 | 23.5 | 5.15 | 90.6 |

W/F=12.5 $g \cdot h \cdot mol^{-1}$, 550 °C, 0.1 MPa, TOS=10 min.

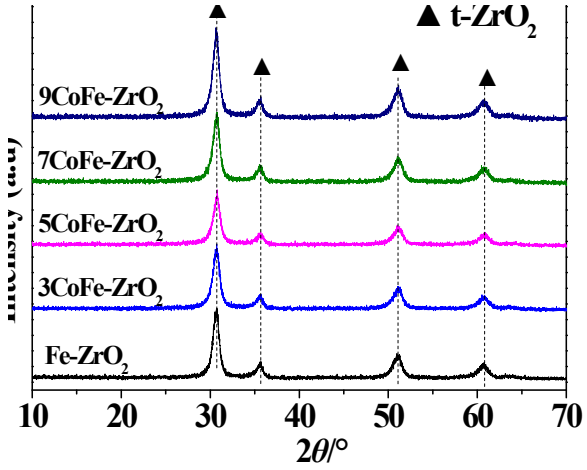


**Fig. S2** XRD patterns of fresh catalysts.

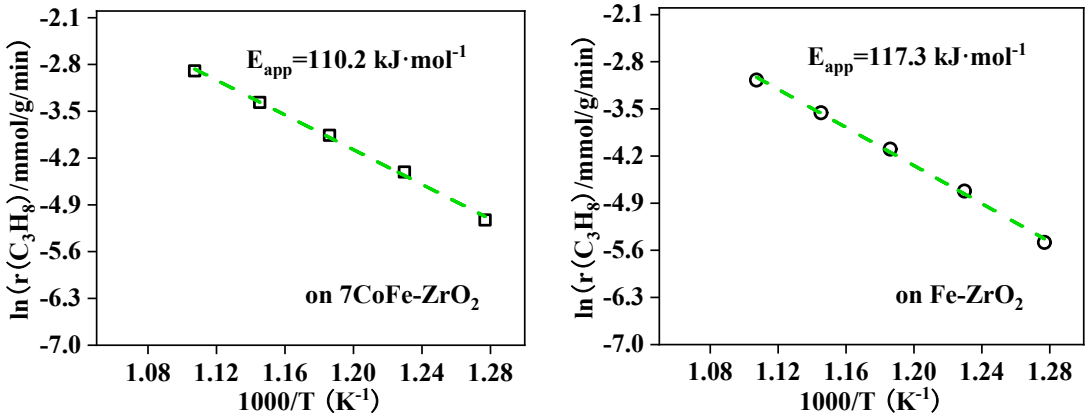


**Fig. S3** Kinetics studies for PDH-$CO_2$.

$F_0$: inlet molar flow rate of $C_3H_8$, X: $C_3H_8$ conversion, and $W_{cat}$: cat. weight (0.5 g).

W/F=5.3 g·h·mol$^{-1}$ (To avoid possible propane pyrolysis).

T=510, 540, 570, 600, and 630 °C, 0.1 MPa.

$$r(C_3H_8)(mmol/g/min)=\frac{F_0 \cdot X(C_3H_8)}{W_{cat}}$$

**Table S3** Electron binding energy of Fe $2p_{3/2}$ for the used catalysts

| Catalysts | B. E. (eV) | | |
|---|---|---|---|
| | $Fe^{2+}$ | $Fe^{3+}$ | $Fe^{2+}$/ $Fe^{3+}$ |
| 7Co-$FeZrO_2$ | 711.4 | 713.5 | 0.52 |
| Fe-$ZrO_2$ | 711.2 | 713.5 | 0.47 |

**Table S4** Surface element composition of fresh catalysts based on XPS

| Catalysts | Fe (wt.%) | Zr (wt.%) | O (wt.%) | Co (wt.%) | $Co/(Fe_2O_3+ZrO_2)$ (mass ratio) | $Co/(Fe_2O_3+ZrO_2)$ (nominal mass ratio) |
|---|---|---|---|---|---|---|
| $Fe\text{-}ZrO_2$ | 8.20 | 22.10 | 69.70 | / | / | / |
| $5CoFe\text{-}ZrO_2$ | 6.63 | 18.48 | 72.74 | 2.15 | 4.87 | 5.0 |
| $7CoFe\text{-}ZrO_2$ | 5.69 | 17.39 | 74.23 | 2.69 | 6.84 | 7.0 |
| $9CoFe\text{-}ZrO_2$ | 4.83 | 16.59 | 75.52 | 3.06 | 8.91 | 9.0 |

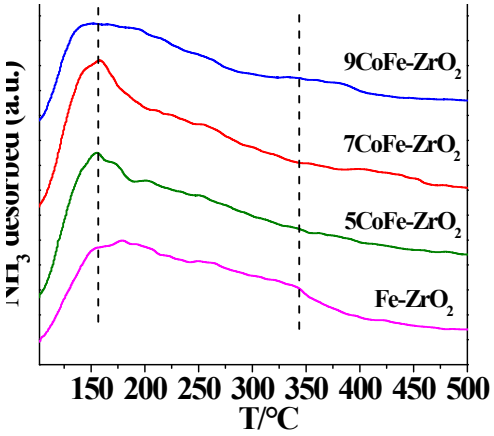


**Fig. S4** $NH_3$-TPD profiles of fresh catalysts.

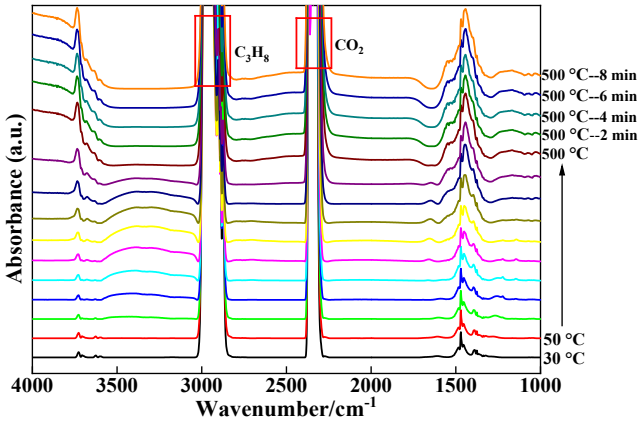


**Fig. S5** *In situ* DRIFT spectra for propane and $CO_2$ reaction on $7CoFe\text{-}ZrO_2$.

**Table S5** *In situ* DRIFT absorption assignments

| Bands | Species | Modes | Ref. |
|---|---|---|---|
| 3734 | M(Fe/Zr/Co)-OH | υ (O-H) | S1, S2 |
| 3700 | M(Fe/Zr/Co)-OH | υ (O-H) | S3, S4 |
| 3679 | M(Fe/Zr/Co)-OH | υ (O-H) | S1, S2, S4 |
| 3631 | triply bridged-OH (Zr-OH-Fe) | υ (O-H) | S5 |
| 3028-2814 | gaseous $C_3H_8$ | υ (C-H) | S6 |
| 2400-2230 | gaseous or $*CO_2$ | υ (C=O) | S7 |
| 1650 | $*HCO_3$ | υ (COO) | S8 |
| 1546 | *OOCH | υ (COO) | S9 |
| 1530 | $*OOCCH_3$ | υ (COO) | S10 |
| 1469 | methylene in $C_3H_8$ | δ ($CH_2$) | S6, S11 |
| 1453 | methyl in $C_3H_8$/$C_3H_6$ | δ ($CH_3$) | S11 |
| 1443 | methyl in $C_3H_6$ | δ ($CH_3$) | S11 |
| 1394 | $*CO_3$ | υ (C=O) | S8 |
| 1375 | methyl in $C_3H_8$/$C_3H_6$ | δ ($CH_3$) | S6 |
| 1070 | $*OCH_3$ | υ (CO) | S12 |
| 1030 | $*CH_3OH$ | υ (CO) | S12 |

**References**

S1 K. Wang, W. Gao, F. Chen, G. Liu, J. Wu, N. Liu, Y. Kawabata, X. Guo, Y. He, P. Zhang, G. Yang and N. Tsubaki, *Appl. Catal. B: Environ.*, 2022, **301**, 120822.

S2 J. Liu, X. Li, Q. Zhao, J. Ke, H. Xiao, X. Lv, S. Liu, M. Tadé and S. Wang, *Appl. Catal. B: Environ.*, 2017, **200**, 297–308.

S3 Z. Zhang, H. Xia, Q. Dai and X. Wang, *Appl. Catal. A: Gen.*, 2018, **557**, 108-118.

S4 L. Francke, E. Durand, A. Demourgues, A. Vimont, M. Daturic and A. Tressaud, *J. Mater. Chem.*, 2003, **13**, 2330–2340.

S5 B. S. Klose, F. C. Jentoft and R. Schlögl, *J. Catal.*, 2005, **233**, 68–80.

S6 S. Song, K. Yang, P. Zhang, Z. Wu, J. Li, H. Su, S. Dai, C. Xu, Z. Li, J. Liu and W. Song, *ACS Catal.*, 2022, **12**, 5997–6006.

S7 L. P .L. Gonçalves, J. Mielby, O. S. G. P. Soares, J. P. S. Sousa, D. Y. Petrovykh, O. I. Lebedev, M. F. R. Pereira, S. Kegnæs and Y. V. Kolen'ko, *Appl. Catal., B: Environ.*, 2022, **312**, 121376.

S8 P. J. Jodłowski, R. J. Jędrzejczyk, D. Chlebda, M. Gierada and J. Łojewska, *J. Catal.*, 2017, **350**, 1–12.

S9 L. Schumacher and C. Hess, *J. Catal*., 2021, **398**, 29–43.

S10 S. M. K. Airaksinen, M. A. Bañares and A. O. I. Krause, *J. Catal.*, 2005, **230**, 507–513.

S11 Y. Qu, T. Zhao, H. Zhao, Z. Zhang and Z. Hao, *Appl. Surf. Sci.*, 2022, **578**, 152067.

S12 Z. Skoufa, E. Heracleous and A. A. Lemonidou, *J. Catal.*, 2015, **322**, 118–129.